Mon. Not. R. Astron. Soc. **371,** 1705–1716 (2006) doi:10.1111/j.1365-2966.2006.10807.x

Absorption of nuclear γ-rays on the starlight radiation in FR I sources: the case of Centaurus A

Ł. Stawarz,[1,2,3]★ F. Aharonian,[2] S. Wagner[1] and M. Ostrowski[3]

[1]*Landessternwarte Heidelberg, Königstuhl, D-69117 Heidelberg, Germany*
[2]*Max-Planck-Institut für Kernphysik, Saupfercheckweg 1, 69117 Heidelberg, Germany*
[3]*Obserwatorium Astronomiczne, Uniwersytet Jagielloński, ul. Orla 171, 30-244 Kraków, Poland*

Accepted 2006 July 11. Received 2006 July 11; in original form 2006 May 30

ABSTRACT

Several BL Lac objects are confirmed sources of variable and strongly Doppler-boosted TeV emission produced in the nuclear portions of their relativistic jets. It is more than probable that also many of the Fanaroff–Riley type I (FR I) radio galaxies, believed to be the parent population of BL Lacs, are TeV sources, for which Doppler-hidden nuclear γ-ray radiation may be only too weak to be directly observed. Here we show, however, that about 1 per cent of the total time-averaged TeV radiation produced by the active nuclei of low-power FR I radio sources is inevitably absorbed and re-processed by photon–photon annihilation on the starlight photon field, and the following emission of the created and quickly isotropized electron–positron pairs. In the case of the radio galaxy Centaurus A, we found that the discussed mechanism can give a distinctive observable feature in the form of an isotropic γ-ray halo. It results from the electron–positron pairs injected to the interstellar medium of the inner parts of the elliptical host by the absorption process, and upscattering starlight radiation via the inverse-Compton process mainly to the GeV–TeV photon energy range. Such a galactic γ-ray halo is expected to possess a characteristic spectrum peaking at $\sim$0.1 TeV photon energies, and the photon flux strong enough to be detected by modern Cherenkov Telescopes and, in the future, by GLAST. These findings should apply as well to the other nearby FR I sources.

Key words: radiation mechanisms: non-thermal – galaxies: active – galaxies: individual: Centaurus A – galaxies: jets – gamma-rays: theory.

1 INTRODUCTION

Centaurus A is the most nearby active galaxy, hosted by a powerful elliptical (see a monograph by Israel 1998). At low frequencies it reveals a giant (8×4 deg or 500×250 kpc) and complex radio structure, with a total 5-GHz energy flux of 3.4×10^{-11} erg cm^{-2} s^{-1}, containing a one-sided kpc-scale jet, few-kpc-long inner lobes and extended outer lobes. The host galaxy is of 14×18 arcmin^2 optical size, has a blue luminosity of $7.5 \times 10^{10}\,L_{\odot}$ and contains a $\sim 10^8\,M_{\odot}$ supermassive black hole in the centre (Marconi et al. 2006). The famous 'dark lane' pronounced within the galactic body, being in fact an edge-on disc of rotating gas, dust and young stars, is most probably a remnant of the merger with a spiral galaxy, which happened some 10^8–10^9 yr ago. The kpc-scale jet and the active nucleus are confirmed sources of X-ray emission (see most recent analysis by Hardcastle et al. 2003; Kataoka et al. 2006, and references therein).

Cen A source is classified as a Fanaroff–Riley type I (FR I) radio galaxy, although some of its morphological characteristics (double–double structure, one-sided jet) are not typical for this class of active galactic nuclei (AGNs). FR I galaxies are believed to be a parent population of BL Lac objects (Urry & Padovani 1995), some of which are confirmed sources of very high-energy (VHE) γ-ray emission. In fact, the nuclear part of the Cen A jet was modelled in terms of a 'misaligned' (and therefore Doppler-hidden) BL Lac, since the jet viewing angle in this source is expected to be much larger than the typical inclination of the blazar jet (e.g. Bailey et al. 1986; Morganti et al. 1991; Botti & Abraham 1993; Steinle et al. 1998; Chiaberge, Capetti & Celotti 2001). As such, Cen A was considered for some time as a potential source of TeV radiation, for which jet misalignment effects are compensated by the source's proximity. This expectation was strengthened by the positive detection of the considered object at MeV–GeV energy range by all the instruments

★E-mail: Lukasz.Stawarz@mpi-hd.mpg.de

onboard *CGRO* during the period 1991–1995 (and references therein Steinle et al. 1998). Nevertheless, the observations performed till now at the TeV energy range resulted in the upper limit for such an emission, only (Rowell et al. 1999; Aharonian et al. 2004, 2005).

In this paper, we investigate the emission resulting from reprocession of the potential γ-ray flux of the active nucleus in the Cen A radio galaxy via annihilation of the nuclear γ-rays on the starlight photon field due to the host galaxy, followed by the synchrotron and inverse-Compton cooling of the created electron–positron pairs. We show that the analysis of this mechanism – which also applies to other FR I sources – can give us interesting constraints on the unknown parameters of the Doppler-hidden and heavily obscured Cen A nucleus, as well as of its host galaxy and outer parts of its radio outflow. We note that the γ-ray opacity in blazar sources was considered before only in the context of nuclear target radiation fields, due to accretion discs, broad-line regions, or dusty tori (e.g. Dermer & Schlickeiser 1994; Sikora, Begelman & Rees 1994; Blandford & Levinson 1995; Wagner et al. 1995; Böttcher, Mause & Schlickeiser 1997; Wang 2000). In the case of the FR I/BL Lac sources, however, such radiation fields are relatively weak, or even absent. Thus, the main source of the opacity for the TeV photons emitted from their active nuclei is the starlight radiation. This radiation can be modelled quite precisely, since all the low-power radio sources of the FR I/BL Lac type are hosted by giant elliptical galaxies (e.g. Colina & de Juan 1995; Urry et al. 2000; Heidt et al. 2004), for which spectral and spatial distribution of the stellar emission is relatively well known (see in this context discussion in Stawarz et al. 2005; Stawarz, Kneiske & Kataoka 2006a; Stawarz et al. 2006b).

Below, in Section 2, we present details regarding the calculation of the optical depth for photon–photon pair production by the Cen A nuclear γ-ray emission on the starlight photon field of the elliptical galaxy, and the energetics of the created electron–positron pairs. In Section 3, we discuss further evolution of such particles injected into the interstellar medium of the elliptical host, calculating in particular the resulting synchrotron and inverse-Compton fluxes. Section 4 contains a final discussion and conclusions.

2 CALCULATIONS

2.1 Opacity

In order to calculate the opacity for the γ-ray photon beam propagating through the galaxy, one has to specify the spectral and spatial distribution of the stellar photon field(s). Starlight surface brightness in elliptical galaxies, including those with active nuclei, are typically well fitted by an empirical Nuker law (Lauer et al. 1995). In terms of monochromatic starlight intensity, this law can be expressed as

$$I(r) = I_{\rm b}\, 2^{(b-d)/a} \left(\frac{r}{r_{\rm b}}\right)^{-d} \left[1 + \left(\frac{r}{r_{\rm b}}\right)^{a}\right]^{-(b-d)/a}, \tag{1}$$

where r is the distance from the galactic nucleus, $r_{\rm b}$ is the 'break' radius and $I_{\rm b} = I(r_{\rm b})$. Such profiles imply a power-law dependence $I(r) \propto r^{-d}$ for $r < r_{\rm b}$, and $I(r) \propto r^{-b}$ at larger distances. de Ruiter et al. (2005) found that in the case of weak radio galaxies (selected from the B2 sample with the criterium of not showing significant dust emission), the host galaxies are characterized by the typical values of $a = 1.9$, $b = 1.6$ and $d = 0.02$. In a specific case of the Cen A host galaxy, Capetti & Balmaverde (2005) gave $a = 1.68$, $b = 1.3$, $d = 0.1$ and a break radius $r_{\rm b} = 2.56\,{\rm arcsec} = 41\,{\rm pc}$. These values are considered hereafter, allowing to approximate the starlight emissivity, $j(r) \propto r^{-1}\, I(r)$, in the NGC 5128 (Cen A host) galaxy, as

$$\epsilon\, j_{\epsilon}(\xi) = j_V\, g(\epsilon)\, h(\xi), \tag{2}$$

where $\xi \equiv r/r_{\rm b}$. Here $\epsilon \equiv \varepsilon/m_{\rm e}\, c^2$ is the starlight photon energy ε in $m_{\rm e}c^2$ units, j_V is the total V-band galactic emissivity, $g(\epsilon)$ describes the V-band normalized spectral distribution of the stellar photon field and

$$h(\xi) = \left(\frac{r}{r_{\rm b}}\right)^{-1} \frac{I(r)}{I_{\rm b}} = 1.64\, \xi^{-1.1}\, (1 + \xi^{1.68})^{-0.7143} \tag{3}$$

is the radial depedance function. The considered galaxy is 14×18 arcmin^2 in optical size (Israel 1998), and hence we take the average terminal galactic radius of 16 arcmin, or $\xi_{\rm t} \equiv r_{\rm t}/r_{\rm b} = 375$, leading to the galactic volume ($\mathcal{V}$) integral

$$\mathcal{H} \equiv \int_{\mathcal{V}} h(\xi)\, {\rm d}\mathcal{V} = 4\pi r_{\rm b}^3 \int_0^{\xi_{\rm t}} \xi^2\, h(\xi)\, {\rm d}\xi = 1.83 \times 10^3\, r_{\rm b}^3 \tag{4}$$

(assuming spherical symmetry). For the spectral distribution of the NGC 5128 starlight, we assume the template spectrum of a powerful elliptical galaxy as provided by Silva et al. (1998), restricted to the photon energy range between $\epsilon_{\rm min} = 10^{-7}$ and $\epsilon_{\rm max} = 10^{-5}$. This restriction implies that we consider only the direct stellar emission of the evolved red giants (constituting the main body of the elliptical host) and their winds, but not the far-infrared emission resulting from the reprocession of the starlight photons by the cold galactic dust (see Appendix A). We normalize it to the V-band radiation, so that $g(\epsilon = h/m_{\rm e}c\lambda_V) = 1$, where $\lambda_V = 0.55\,\mu{\rm m}$. The resulting spectral function $g(\epsilon)$ is shown in Fig. 1 (top panel): values read directly from Silva et al. (1998) are represented by crosses, and the broken power-law approximation considered hereafter,

$$g(\epsilon) = \begin{cases} 2.67 \times 10^{14}\, \epsilon^{2.44} & \text{for} \quad 10^{-7.0} \leqslant \epsilon \leqslant 10^{-5.8} \\ 9.25 \times 10^{-4}\, \epsilon^{-0.57} & \text{for} \quad 10^{-5.8} < \epsilon < 10^{-5.3} \\ 3.54 \times 10^{-31}\, \epsilon^{-5.74} & \text{for} \quad 10^{-5.3} \leqslant \epsilon \leqslant 10^{-5.0} \end{cases} \tag{5}$$

is shown as a solid line.

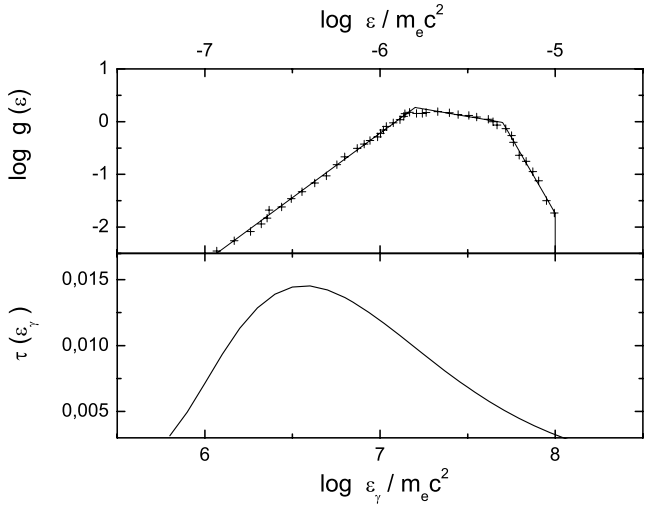

Figure 1. Top panel: spectral energy distribution of the starlight emission of a template giant elliptical host; values read directly from Silva et al. (1998) are represented by crosses, and the broken power-law approximation introduced in this paper is shown as a solid line. Bottom panel: optical depth for annihilation of the nuclear γ-ray emission on the starlight photon field.

The apparent V-band magnitude of NGC 5128 is $m_V = 6.98$ (Israel 1998). This gives the monochromatic V-band galactic luminosity as

$$\log\left(\frac{L_V}{\mathrm{erg/s}}\right) = 50.078 + 2\,\log\left(\frac{d_\mathrm{L}}{\mathrm{Mpc}}\right) - 0.4\,(m_V - A_V) - c_V = 43.82, \tag{6}$$

where the distance of CenA is $d_\mathrm{L} = 3.4$ Mpc, the extinction is $A_V = 0.381$ and $c_V = 4.68$. Since, by the definition,

$$L_V = 4\pi \int_{\mathcal{V}} [\epsilon\, j_\epsilon(\xi)]_V \,\mathrm{d}\mathcal{V} = 4\pi\, j_V\, \mathcal{H}, \tag{7}$$

one obtains $j_V = 1.42 \times 10^{-21}$ erg cm^{-3} ster^{-1} s^{-1}. Note, that by means of standard radiative transfer formulae, the spectral intensity within a solid angle Ω, which can be obtained by integrating spectral emissivity along a ray as $I_\nu(\Omega) = \int\, j_\nu(\xi)\,\mathrm{d}l$, is related to the differential photon number density, $n_\epsilon(\xi, \Omega)$, through the expression $I_\nu(\Omega) = ch\,\epsilon\, n_\epsilon(\xi, \Omega)$. This corresponds in fact to the neglegible absorption of the starlight along the light path, the approximation which may be considered as being in conflict with the presence of the dust lane in Cyg A host. It is, however, good enough for the purpose of the presented evaluation, since integration over the whole extended elliptical volume reduces the starlight absorption effects. As a result,

$$n_\epsilon(\xi, \Omega) = \frac{\epsilon^{-2}}{m_\mathrm{e} c^3} \int [\epsilon\, j_\epsilon(\xi)]\,\mathrm{d}l. \tag{8}$$

The optical depth for photon–photon annihilation, computed for the case of a monodirectional beam of γ-ray photons with a dimensionless energy ϵ_γ, propagating through the stellar photon field of the host galaxy from the active centre up to the terminal distance r_t, is

$$\tau(\epsilon_\gamma) = \int_0^{r_\mathrm{t}} \mathrm{d}r \int \mathrm{d}n\,(1 - \varpi)\,\sigma_{\gamma\gamma}, \tag{9}$$

where ϖ is the cos function of the angle between the γ-ray photon and the incident starlight photon, $\mathrm{d}\,n = n_\epsilon(\xi, \Omega)\,\mathrm{d}\,\epsilon\,\mathrm{d}\,\Omega$ is the differential starlight photon number density, and

$$\sigma_{\gamma\gamma}(\epsilon_\gamma, \epsilon, \varpi) = \frac{3\sigma_\mathrm{T}}{16}\,(1 - \beta^2)\,\left[(3 - \beta^4)\,\ln\left(\frac{1+\beta}{1-\beta}\right) - 2\beta\,(2 - \beta^2)\right] \tag{10}$$

is the photon–photon annihilation cross-section (Gould & Schréder 1967), where

$$\beta \equiv \left[1 - \frac{2}{\epsilon_\gamma \epsilon\,(1 - \varpi)}\right]^{1/2} \tag{11}$$

is the velocity of the created electron/positron (computed via the conservation of four-momentum) in the appropriate centre-of-momentum frame. By choosing $\mathrm{d}\Omega = \mathrm{d}\phi\,\mathrm{d}\varpi$, the differential starlight photon number density (see equation 8) reads as

$$n_\epsilon(\xi, \Omega) = \frac{\epsilon^{-2}\, r_\mathrm{b}}{m_\mathrm{e} c^3} \int_0^{\eta_\mathrm{max}} [\epsilon\, j_\epsilon(\zeta)]\,\mathrm{d}\eta, \tag{12}$$

where $\eta \equiv l/r_\mathrm{b}$, $\zeta = \sqrt{\xi^2 + \eta^2 - 2\xi\eta\varpi}$ and the integration upper limit is $\eta_\mathrm{max} = \xi\varpi + \sqrt{\xi^2\varpi^2 - \xi^2 + \xi_\mathrm{t}^2}$. This gives finally

$$\tau(\epsilon_\gamma) = \frac{2\pi\, j_V\, r_\mathrm{b}^2}{m_\mathrm{e}\, c^3} \int_{-1}^{+1} \mathrm{d}\varpi\,(1 - \varpi) \int_{\max(\epsilon_\mathrm{min}, \epsilon_\mathrm{thre})}^{\epsilon_\mathrm{max}} \mathrm{d}\epsilon\,\sigma_{\gamma\gamma}(\epsilon_\gamma, \epsilon, \varpi)\,\frac{g(\epsilon)}{\epsilon^2} \int_0^{\xi_\mathrm{t}} \mathrm{d}\xi \int_0^{\eta_\mathrm{max}} \mathrm{d}\eta\, h(\zeta), \tag{13}$$

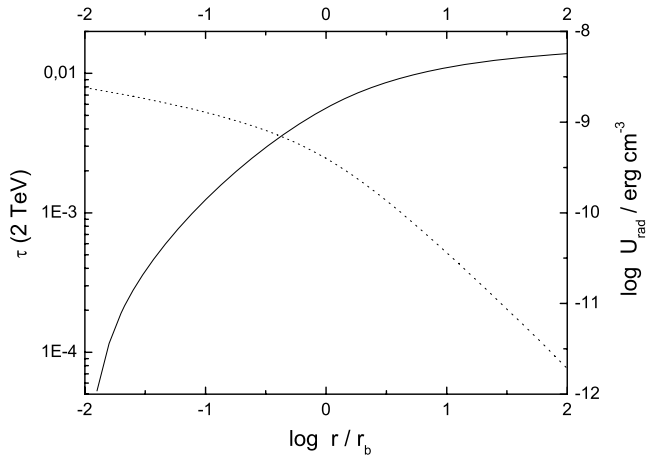

Figure 2. Left-hand panel: optical depth for 2-TeV photons as a function of the distance from the active nucleus (solid line). Right-hand panel: profile of the energy density of the starlight photon field (dotted line).

where the threshold energy is $\epsilon_{\rm thre} = 2/\epsilon_\gamma\,(1-\varpi)$. This optical depth as a function of the γ-ray photon energy is shown in Fig. 1 (bottom panel). As can be seen, it possesses a broad maximum at $\varepsilon_\gamma \approx 1-10$ TeV, with the maximum value $\tau(2\,{\rm TeV}) \approx 0.0145$.

Let us fix the γ-ray photon energy at $\epsilon_\gamma = 10^{6.6}$, and compute again the appropriate optical depth for photon–photon annihilation as a function of the upper bound in integration over the distance from the core, $\tau = \tau(\xi)$, replacing simply constant $\xi_{\rm t}$ in equation (13) with variable ξ. Such a profile is shown in Fig. 2 (solid line): as can be seen, only about 40 per cent ($\tau \approx 0.006$) of the annihilated radiation is in fact absorbed within the innermost galactic volume of radius $r_{\rm b}$, and the remaining 60 per cent is absorbed at distances $r_{\rm b} < r < 100\,r_{\rm b}$. The obtained profile for τ can be compared with the spatial distribution of the galactic radiation. Noting the definition for the photon field spectral energy density,

$$U_\nu = \frac{2\pi}{c}\int_{-1}^{+1} I_\nu(\Omega)\,{\rm d}\varpi, \tag{14}$$

one may find the appropriate bolometric energy density profile for the starlight emission as

$$U_{\rm rad}(\xi) = f_{\rm bol}\,[\nu U_\nu]_V = f_{\rm bol}\,\frac{2\pi r_{\rm b}\,j_V}{c}\int_{-1}^{+1}{\rm d}\varpi\int_0^{\eta_{\rm max}}{\rm d}\eta\;h(\zeta), \tag{15}$$

where $f_{\rm bol} = 2.5$ is the V-band bolometric correction for the adopted here stellar spectrum (equation 5). This profile is shown in Fig. 2 as a dotted line.

The spectral and spatial shapes of the optical depth for the photon–photon annihilation discussed above for the Cen A radio galaxy is universal, and should hold also for the other low-power radio sources hosted by elliptical galaxies. That is caused by the appropriate scaling $\tau \propto j_V\,r_{\rm b}^2$ (equation 13), $j_V \propto L_V/\mathcal{H}$ (equation 7) and $\mathcal{H} = \kappa r_{\rm b}^3$ (equation 4), where $\kappa = \kappa(a, b, d)$ is a numerical factor depending on the parameters of the Nuker profile (e.g. $\kappa = 1.83\times10^3$ in the case of NGC 5128, as given in equation 3). These relations give $\tau \propto L_V/\kappa r_{\rm b}$. Since the parameters of the NGC 5128 Nuker profile ($a = 1.68, b = 1.3, d = 0.1$ Capetti & Balmaverde 2005) are similar to the average hosts of B2 radio sources ($a = 1.9, b = 1.6$ and $d = 0.02$; de Ruiter et al. 2005), since the spectral energy distribution of the starlight emission considered here is based on a universal spectrum of the elliptical galaxy (Silva et al. 1998), and since the break radius scales linearly with the V-band galactic luminosity,

$$\left(\frac{r_{\rm b}}{\rm kpc}\right) \approx \left(\frac{L_V}{10^{45}\,{\rm erg\,s^{-1}}}\right) \tag{16}$$

(de Ruiter et al. 2005), the optical depth for the γ-ray photons shown in Figs 1 and 2 for the case of Cen A radio galaxy indeed should apply also to the other analogous sources. We note, for example, that with the value of L_V found previously for the NGC 5128 galaxy, the simple scaling introduced in equation (16) implies the break radius ≈66 pc, which is very close to the observed value of $r_{\rm b} \approx 41$ pc (Capetti &

Balmaverde 2005). On the other hand, the starlight energy density profile $U_{\rm rad} \propto j_V r_{\rm b} \propto r_{\rm b}^{-1}$ is supposed to change for different sizes (and hence luminosities) of the elliptical host when compared with the particular profile shown in Fig. 2 for the case of NGC 5128 parameters.

2.2 Energetics

The obvious source of γ-ray photons in the Cen A system is the active nucleus (containing a relativistic jet), which is most probably responsible for the production of the flux detected by OSSE (0.05–4 MeV), COMPTEL (0.75–30 MeV) and EGRET (0.1–1.0 GeV) instruments onboard *CGRO* in the period 1991–1995, with the total observed 50 keV–1 GeV luminosity $\sim 3 \times 10^{42}$ erg s^{-1} (and references therein Steinle et al. 1998). This emission peaks at $\approx$0.1 MeV, with the maximum energy flux about $\sim 10^{-9}$ erg cm^{-2} s^{-1}. At a very high γ-ray energy range, a 3σ detection of Cen A with the photon flux $F(>0.3\,{\rm TeV}) = 4.4 \times 10^{-11}$ ph cm^{-2} s^{-1} was reported in the seventies (Grindlay et al. 1975). Subsequent CANGAROO observations resulted in the upper limit $F(>1.5\,{\rm TeV}) < 5.45 \times 10^{-12}$ ph cm^{-2} s^{-1} for the point source centred at the Cen A nucleus, and $F(>1.5\,{\rm TeV}) < 1.28 \times 10^{-11}$ ph cm^{-2} s^{-1} for the extended region with radius 14 arcmin (Rowell et al. 1999). The most recent HESS observations gave $F(>0.19\,{\rm TeV}) < 5.68 \times 10^{-12}$ ph cm^{-2} s^{-1} for the point-like active nucleus (Aharonian et al. 2005).

Here, we are interested in the total, time- and angle-averaged (i.e. 'calorimetric') flux of TeV photons produced by the active nucleus and 'injected' into the host galaxy as well as into the large-scale radio structure. With the most recent HESS results, we can only put some upper limits for it. Namely, assuming a standard spectral index $\alpha_\gamma = 1$ (equivalent to the photon index $\Gamma_\gamma = \alpha_\gamma + 1 = 2$) at the considered photon energy range, the relation between the integrated photon flux and the monochromatic flux energy density at any photon energy $\varepsilon \geqslant \varepsilon_0$ is simply $[\varepsilon S_\varepsilon] = [\varepsilon_0 F(>\varepsilon_0)]$. This flux is related to the emitting fluid (jet) intrinsic monochromatic power (assumed to be isotropic in the jet comoving frame) radiated in a given direction, $\partial L'/\partial\, \Omega' = L'/4\,\pi$, by the expression

$$[\nu S_\nu] = \frac{1}{d_{\rm L}^2}\,\frac{\delta_{\rm nuc}^3}{\Gamma_{\rm nuc}}\,\frac{\partial L'}{\partial \Omega'} = \frac{1}{d_{\rm L}^2}\,\frac{\delta_{\rm nuc}^3}{\Gamma_{\rm nuc}}\,\frac{L'}{4\pi}, \tag{17}$$

where $\Gamma_{\rm nuc}$ and $\delta_{\rm nuc} = \Gamma_{\rm nuc}^{-1}\,(1 - \sqrt{1-\Gamma_{\rm nuc}^{-2}}\cos\theta)^{-1}$ are, respectively, Lorentz and Doppler factors of the nuclear portion of the jet, and θ is the jet viewing angle (e.g. Sikora et al. 1997; Stawarz, Sikora & Ostrowski 2003). On the other hand, the total power radiated into the ambient medium being of interest here, is

$$L_{\rm inj} = \oint \frac{\delta_{\rm nuc}^3}{\Gamma_{\rm nuc}}\,\frac{\partial L'}{\partial \Omega'}\,{\rm d}\Omega = \frac{1}{2}\,L'\,\Gamma_{\rm nuc}^{-1}\int_0^\pi \delta_{\rm nuc}^{-3}\,\sin\theta\,{\rm d}\theta = L', \tag{18}$$

and hence

$$L_{\rm inj} = 4\pi\, d_{\rm L}^2\,\Gamma_{\rm nuc}\delta_{\rm nuc}^{-3}\,[\varepsilon_0\,F(>\,\varepsilon_0)]. \tag{19}$$

With the HESS photon flux $F(>0.19\,{\rm TeV}) < 5.68 \times 10^{-12}$ ph cm^{-2} s^{-1} (corresponding to the few-arcmin-integration area centred on the Cen A nucleus) one obtains the upper limit for the total injected monochromatic power $L_{\rm inj} < 2.4 \times 10^{39}\,\Gamma_{\rm nuc}\,\delta_{\rm nuc}^{-3}$ erg s^{-1}. With the preferred values $\theta \sim 50$–80° inferred from the VLBI radio observations (Jones et al. 1996; Tingay et al. 1998), and $\Gamma_{\rm nuc} \sim 10$ widely considered as a typical value for the bulk Lorentz factor of subparsec-scale AGN jets, this reads as $L_{\rm inj} < 10^{42}$–10^{43} erg s^{-1}. Below we take conservatively $L_{\rm inj} = 10^{42}$ erg s^{-1} as an upper limit, noting that such a luminosity would correspond to less than 10 per cent of the minimum total kinetic power of the Cen A jet, estimated to be $L_{\rm j} \gtrsim 10^{43}$ erg s^{-1} from the radio/X-ray lobes' energetic (see Clarke, Burns & Norman 1992; Kraft et al. 2003). As shown in the previous section, about 1 per cent of this power is absorbed on the starlight photon field within the central $100\,r_{\rm b} \sim 4$ kpc region of the host galaxy, and is thus converted to an electron–positron population, mainly in the 0.1–1 TeV energy range.

The nuclear γ-ray emission postulated here is expected to be Doppler-boosted within the narrow cone characterized by the opening angle $\Gamma_{\rm nuc}^{-1} \lesssim 6^\circ$. Therefore, it is strongly Doppler hidden when viewed from $\theta \geqslant 50^\circ$ (see equation 17). If the observer was located within the beaming cone of this emission, however, he would detect a flux corresponding to the isotropic luminosity $L(0) = (\delta_{{\rm nuc},\,\theta=0}^3/\Gamma_{\rm nuc})\,L' \approx \Gamma_{\rm nuc}^2\,L' < 10^{44}$ erg s^{-1}. Such values are consistent with luminosities observed from the TeV-detected BL Lac objects (see, e.g. Katarzyński et al. 2006), which are believed to be beamed analogues of the low-power FR I radio galaxies like Cen A (Urry & Padovani 1995).

In order to find the energy spectrum of the created electrons and positrons, we note that the pair production rate for small values of the optical depth can be estimated as

$$Q(\gamma, r) \propto \left[n_\gamma(\epsilon_\gamma) \times \frac{{\rm d}\tau(\epsilon_\gamma)}{{\rm d}r}\right]\Bigg|_{\epsilon_\gamma = 2\,\gamma} \tag{20}$$

(e.g. Coppi & Blandford 1990; Böttcher & Schlickeiser 1997), where γ is the Lorentz factor of the created particles, and $n_\gamma(\epsilon_\gamma)$ is the photon spectrum of the primary γ-ray photons. For the latter we assume power-law form $n_\gamma(\epsilon_\gamma) \propto \epsilon_\gamma^{-\Gamma_\gamma}$, where $\Gamma_\gamma = \alpha_\gamma + 1$ is the photon index. When averaged over the galactic radius, the pair production rate therefore scales as

$$Q(\gamma) \propto \gamma^{-\Gamma_\gamma}\,\tau\,(2\,\gamma)\,. \tag{21}$$

This function is shown in Fig. 3 in normalized units (open circles) for $\Gamma_\gamma = 2$, taken in this paper as a typical photon index of blazars' TeV emission. As illustrated, $Q(\gamma)$ is peaked at $\gamma \sim 10^{5.5}$, and decreases as $\propto \gamma^{-(\Gamma_\gamma + 0.5)}$ for $\gamma > 10^6$. Such behaviour is in fact expected, since for $\epsilon_\gamma > 10^{6.6}$ the optical depth evaluated previously is roughly $\tau(\epsilon_\gamma) \propto \epsilon_\gamma^{-0.5}$. Fig. 3 shows also the pair injection energy distribution calculated using the expression introduced by Aharonian, Atoyan & Nagapetyan (1983, solid line), integrated over the spatial-averaged spectrum of the starlight photons (equation 12; see also equation 34 below) and the assumed photon spectrum of primary γ-rays, $\propto \epsilon_\gamma^{-2}$. We note that the

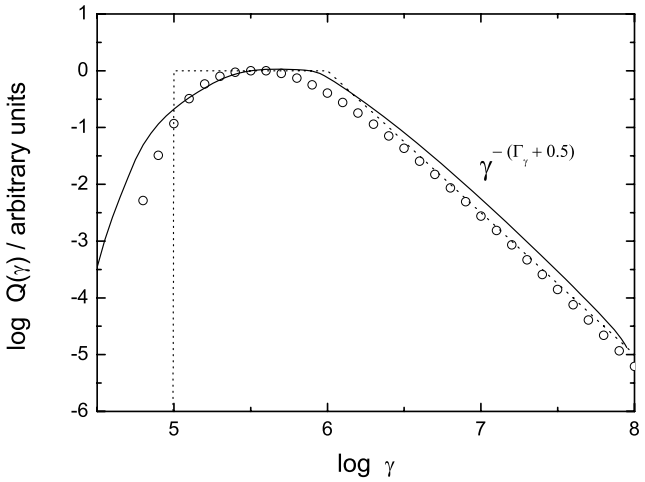

Figure 3. Different approximations for the pair injection energy spectrum (corresponding to the photon flux of the primary γ-rays $\propto \epsilon_\gamma^{-2}$) in normalized units: (i) $Q(\gamma) \propto \gamma^{-2}\,\tau(2\,\gamma)$ (open circles), (ii) $Q(\gamma)$ calculated using the pair production rate expression introduced by Aharonian et al. (1983, solid line) and (iii) broken power-law approximation introduced in this paper (dotted line).

approximation of Aharonian et al. (1983) for the energy distribution of the secondary electrons provides accuracy better than a few per cent (see detailed calculations in Böttcher & Schlickeiser 1997). Small differences between the two presented estimates come from the fact that the function given by Aharonian et al. (1983) corresponds to the isotropic distribution of the soft photons, while the optical depth calculated by us (i.e. equations 20 and 21) includes the anisotropy of the starlight radiation field. Finally, Fig. 3 shows also the simplest broken power-law approximation for the injection pair spectrum considered hereafter for the purpose of the following calculations: $Q(\gamma) \propto$ constant for $\gamma_0 \equiv 10^5 \leqslant \gamma \leqslant \gamma_{\rm br} \equiv 10^6$, and $Q(\gamma) \propto \gamma^{-2.5}$ for $\gamma > \gamma_{\rm br}$. We normalize it to the monochromatic 1-TeV power $L_{\rm inj}$ specified above, to obtain

$$Q(\gamma) = \frac{\tau\, L_{\rm inj}\, \mathcal{I}(\gamma)}{\gamma_{\rm br}^2\, m_{\rm e} c^2\, \mathcal{V}_{\rm gal}} \quad \text{where} \quad \mathcal{I}(\gamma) = \begin{cases} 1 & \text{for} \quad \gamma_0 \leqslant \gamma \leqslant \gamma_{\rm br} \\ (\gamma_{\rm br}/\gamma)^{2.5} & \text{for} \quad \gamma > \gamma_{\rm br} \end{cases} \tag{22}$$

and zero otherwise. Here $\tau \equiv \tau(\epsilon_\gamma = 1\,{\rm TeV}) \approx 0.01$, and $\mathcal{V}_{\rm gal}$ is the galactic volume in which the pair injection is taking place.

3 IMPLICATIONS

The electrons and positrons produced by annihilation of the VHE γ-ray nuclear photons on starlight radiation are expected to have an initial spectrum peaked at 0.1–1 TeV energies. After being injected into the galactic medium, they are quickly isotropized by the ambient magnetic field, and radiate via the synchrotron and inverse-Compton processes. The evolution of these electrons and details of their emission spectra depend therefore on the properties of the interstellar medium of the elliptical host.

3.1 Elliptical host

Moss & Shukurov (1996) argued that elliptical galaxies have no ordered large-scale magnetic field, but only an unresolved random component. They further suggested that the latter is due to a 'fluctuation dynamo' driven by the turbulent motions of the interstellar matter caused by Type I supernovae and stellar motions. The latter ones are expected to be characterized by the Kolmogorov-like energy spectrum and an injection scale $\sim$3 pc, while the former ones by a steeper (shock-like) spectrum and larger injection scale, $\sim$300 pc. The resulting random magnetic field is expected to be characterized by the average galactic intensity $\sim$3 μG (reaching $\sim$10 μG in the central parts) and the correlation scale $\sim$100 pc. Moss & Shukurov (1996) demonstrated that their model is consistent with all the observational constraints (in particular with the depolarization studies). In the case of Centaurus A, and in general all the ellipticals hosting radio-loud AGNs, a galactic magnetic field can be even higher than this, especially close to the galactic centre, possessing even some regular component due to pollution of the interstellar medium by the magnetized plasma transported from the active core in the form of the jets. However, for the purpose of order-of-magnitude evaluations, below we take the characteristic values for the NGC 5128 elliptical host's magnetic field $B_{\rm gal} \approx 3$–10 μG, assuming that it consists solely of the (Alfvénic) turbulent component with the maximum wavelength $\lambda_{\rm max} \sim 100$ pc and the Kolmogorov energy spectrum $W(k) \propto k^{-q}$, where $q = 5/3$.

With the interstellar medium parameters as discussed above, the mean free path of the created electron–positron pairs for resonant interactions with the turbulent Alfvèn modes, is (Schlickeiser 1989):

$$\lambda_{\rm e} \approx r_{\rm g} \left(\frac{\lambda_{\rm max}}{r_{\rm g}}\right)^{q-1} = r_{\rm g}^{1/3}\, \lambda_{\rm max}^{2/3} \sim 0.82 \times \gamma_6^{1/3}\, B_{-5}^{-1/3}\,{\rm pc}, \tag{23}$$

where $\gamma_6 \equiv \gamma/10^6, r_{\rm g} \equiv \gamma m_{\rm e} c^2/eB_{\rm gal} \sim 5.5 \times 10^{-5}\,\gamma_6 B_{-5}^{-1}$ pc is the electrons' gyroradius, and $B_{-5} \equiv B_{\rm gal}/10\,\mu{\rm G}$ (as a general reference

for the particle–turbulent wave interactions see Schlickeiser 2002). Such interactions lead to quick isotropization of the injected electrons. In particular, the appropriate isotropization time-scale, $t_{\rm iso} \sim 3\,\lambda_{\rm e}/c \sim 8\,\gamma_6^{1/3}\,B_{-5}^{-1/3}$ yr, is a few orders of magnitude shorter than the radiative cooling time-scale (see below). The diffusive escape time-scale from the central parts of the elliptical host ($R \sim 100\,r_{\rm b} \sim 4$ kpc) is $t_{\rm esc} \sim 3\,R^2/\lambda_{\rm e}\,c \sim 2 \times 10^8\,\gamma_6^{-1/3}\,B_{-5}^{1/3}$ yr. We note that the re-acceleration of the radiating particles by resonant scattering on the Alfvèn modes is not expected to be efficient enough to keep the electrons around $\gamma \sim 10^6$. In particular, the time-scale for this process, $t_{\rm acc} \sim \beta_{\rm A}^{-2}\,t_{\rm iso} \sim 4.5 \times 10^6\,\gamma_6^{1/3}\,B_{-5}^{-7/3}$ yr, is much longer than the radiative cooling time-scale. In the above, $v_{\rm A} \equiv \beta_{\rm A}\,c \approx B_{\rm gal}\,(4\,\pi\,m_{\rm p}\,n_{\rm gas})^{-1/2} \sim 10^{-3}\,B_{-5}\,c$ is the Alfvèn velocity expected for the average number density of the cold gas within central (<4 kpc) parts of the NGC 5128 galaxy $n_{\rm gas} \sim 3 \times 10^{-3}$ cm^{-3}. In this context, we note that the most recent analysis presented by Kraft et al. (2003) indicates that the hot gaseous component of the galaxy discussed here is characterized by a temperature $kT \sim 0.3$ keV and a central number density $\sim 4 \times 10^{-2}$ cm^{-3}, which is roughly constant within the radius $r \sim 0.5$ kpc and decreases further away as $\propto r^{-1.2}$. Such a behaviour is consistent with general properties of the elliptical galaxies (Mathews & Brighent 2003). Thus, one can conclude that the TeV energy electrons injected into the interstellar medium (via annihilation of the γ-ray emission of the active centre) are effectively confined to the elliptical body and quickly isotropized by the galactic magnetic field, and therefore radiate all their energy there by inverse-Compton upscattering of the starlight photons and the synchrotron process (see below), before being re-accelerated by the turbulent processes. As a result, one should expect formation of a small-scale (galactic) version of the 'isotropic pair haloes' discussed by Aharonian, Coppi & Völk (1994), restricted, however, to the first generation of the secondary photons.

Below we investigate in more detail the emission spectrum of electron–positron pairs created within the central $100\,r_{\rm b}$ parts of the elliptical host's interstellar medium due to annihilation of the nuclear VHE γ-rays on the starlight photon field. First, we introduce the *averaged* energy density of the starlight photon field, assumed in this section to be isotropic within $100\,r_{\rm b}$,

$$\epsilon U_\epsilon \approx \langle [\nu U_\nu]_V \rangle_\xi \times g(\epsilon) \tag{24}$$

(see equations 5 and 15), where

$$\langle [\nu U_\nu]_V \rangle_\xi \equiv \frac{\int_0^{\xi_{\rm cr}} {\rm d}\xi\,[\nu U_\nu]_V}{\int_0^{\xi_{\rm cr}} {\rm d}\xi} = \frac{2\pi\,r_{\rm b}\,j_V}{c\,\xi_{\rm cr}} \int_0^{\xi_{\rm cr}} {\rm d}\xi \int_{-1}^{+1} {\rm d}\varpi \int_0^{\eta_{\rm max}} {\rm d}\eta\; h(\zeta), \tag{25}$$

and $r_{\rm cr} \equiv \xi_{\rm cr}\,r_{\rm b}$ is some particular critical radius over which the averaging is performed. The total averaged starlight energy density is

$$\langle U_{\rm rad} \rangle = \int_{\epsilon_{\rm min}}^{\epsilon_{\rm max}} U_\epsilon\,{\rm d}\epsilon = f_{\rm bol}\,\langle [\nu U_\nu]_V \rangle_\xi . \tag{26}$$

With $\xi_{\rm cr} = 100$ and other parameters as given above, one obtains $\langle [\nu U_\nu]_V \rangle_\xi \approx 10^{-11}$ergcm^{-3}, and $\langle U_{\rm rad} \rangle \approx 2.5 \times 10^{-11}$ erg cm^{-3}, which is still much higher than the energy density of the galactic magnetic field, $U_{\rm B} = B_{\rm gal}^2/8\pi \approx 4 \times 10^{-12}\,B_{-5}^2$ erg cm^{-3}. The time-scale for the radiative losses of the electrons with Lorentz factor γ, including synchrotron and inverse-Compton losses (in both Thomson and Klein–Nishina regimes) can be then estimated as

$$t_{\rm rad}(\gamma) = \frac{3\,m_{\rm e}c}{4\,\sigma_{\rm T}\,U_{\rm B}\,\gamma\,(1 + q\,F_{\rm KN})}, \tag{27}$$

where $q \equiv \langle U_{\rm rad} \rangle / U_{\rm B} \approx 7\,B_{-5}^{-2}$, and

$$F_{\rm KN} = \frac{1}{\langle U_{\rm rad} \rangle} \int \frac{U_\epsilon}{(1 + 4\,\gamma\,\epsilon)^{1.5}}\,{\rm d}\epsilon \tag{28}$$

(Moderski et al. 2005). The simplified form of the function $F_{\rm KN}$ introduced above is in fact a very accurate approximation for the values $4\,\gamma\epsilon < 4\gamma_{\rm inj}\epsilon_{\rm max} \lesssim 100$, as considered in this paper (with $\epsilon_{\rm max} = 10^{-5}$). The time-scale $t_{\rm rad}(\gamma)$, together with the turbulent re-acceleration time-scale and the escape time-scale, is shown in Fig. 4 as a function of the electron Lorentz factor γ for the range of $B_{\rm gal} = 3$–10 μG [note that $t_{\rm iso}(\gamma)$, not shown in this figure, is much shorter than any other of the time-scales plotted]. As can be seen, $t_{\rm esc} \gg \max\,(t_{\rm acc}, t_{\rm rad})$ for all $\gamma \leqslant \gamma_{\rm br}$, and $t_{\rm acc} \gg t_{\rm rad}$ for $\gamma > \gamma_0$. All the electrons with Lorentz factors $\gamma < \gamma_{\rm KN} \equiv 1/4\,\epsilon_{\rm max} \sim 10^{4.5}$ cool mainly via the inverse-Compton losses in the Thomson regime. Meanwhile, the electrons with $\gamma_{\rm KN} < \gamma < \gamma_{\rm cr}$, where $q\,F_{\rm KN}(\gamma_{\rm cr}) \equiv 1$, lose their energy mainly via the inverse-Compton emission in the Klein–Nishina regime. In the case of $B_{\rm gal} = 3$ μG, one has $\gamma_{\rm cr} \sim \gamma_{\rm br}$, while for $B_{\rm gal} = 10$ μG the critical electron Lorentz factor $\gamma_{\rm cr}$ is a factor of a few lower than that. Finally, the main process responsible for the cooling of the electrons with $\gamma > \gamma_{\rm cr}$ is synchrotron radiation.

The resulting electron energy distribution, $n_{\rm e}(\gamma)$, ignoring re-acceleration and escape effects, can be found from the continuity equation

$$\frac{\partial n_{\rm e}(\gamma)}{\partial t} = -\frac{\partial}{\partial \gamma}\,[|\dot{\gamma}|_{\rm cool}\,n_{\rm e}(\gamma)] + Q(\gamma), \tag{29}$$

where $Q(\gamma)$ denotes injection of high-energy electrons through photon–photon annihilation, and $|\dot{\gamma}|_{\rm cool} = |\dot{\gamma}|_{\rm syn} + |\dot{\gamma}|_{\rm ic}$ is the total rate of the radiative cooling. The standard formulae give

$$|\dot{\gamma}|_{\rm syn} = \frac{4\,c\sigma_{\rm T}}{3\,m_{\rm e}c^2}\,U_{\rm B}\,\gamma^2, \quad \text{and} \quad |\dot{\gamma}|_{\rm ic} = \frac{4\,c\sigma_{\rm T}}{3\,m_{\rm e}c^2}\,U_{\rm B}\,\gamma^2\,q\,F_{\rm KN} \tag{30}$$

(Moderski et al. 2005). Note that for the parameters considered here and electron Lorentz factor $\gamma = 10^6$, the relative importance of the inverse-Compton and synchrotron energy losses, $|\dot{\gamma}|_{\rm ic}/|\dot{\gamma}|_{\rm syn} = q\,F_{\rm KN}$, is roughly $\sim$3 for $B_{\rm gal} = 3$ μG, and $\sim$0.3 for 10 μG. Thus, the energy injected into the created pairs is re-radiated via their synchrotron and inverse-Compton (in the Klein–Nishina regime) processes in roughly

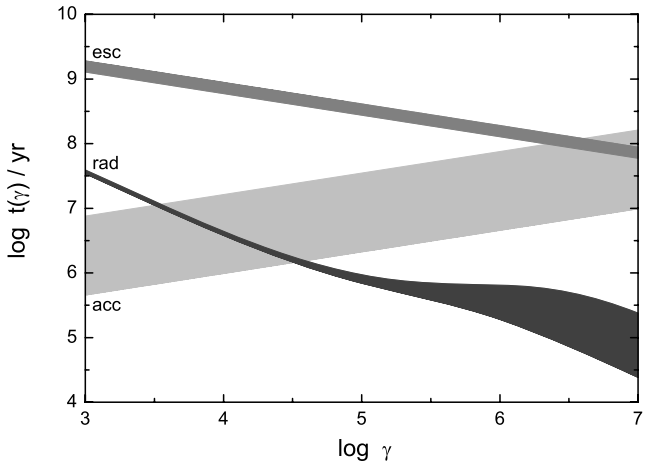

Figure 4. Time-scales for the radiative cooling (dark-grey line), turbulent re-acceleration (light-grey line) and diffusive escape (grey line) of the electrons injected into the interstellar medium of the elliptical host, for the range of the galactic magnetic field 3–10 μG. The values corresponding to $B_{\rm gal} = 10\,\mu$G correspond to the lower bounds for the radiative losses and the acceleration time-scales, and to the upper bound for the escape time-scales, respectively.

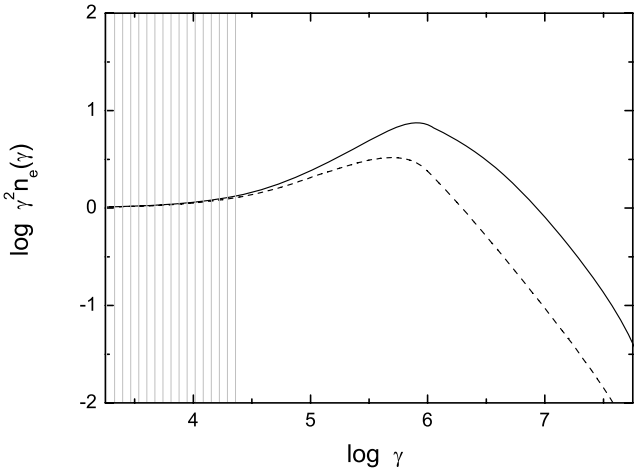

Figure 5. Energy distribution of the electrons injected to the interstellar medium of the elliptical host, for the galactic magnetic field 3 μG (solid line) and 10 μG (dashed line), in normalized units. Shaded region indicates the electrons' energy range in which neglected re-acceleration effects are expected to become important.

comparable amounts. As for the function $Q(\gamma)$, we use approximation for the electrons freshly injected to the galactic volume $\mathcal{V}_{\rm gal}$ introduced by equation (22), to obtain the steady-state solution

$$n_{\rm e}(\gamma) = \frac{3\,m_{\rm e}c}{4\,\sigma_{\rm T}}\,\frac{\int_{\gamma}\,{\rm d}\gamma'\,Q(\gamma')}{\gamma^2\,U_{\rm B}\,(1+q\,F_{\rm KN})} = \frac{3\tau L_{\rm inj}}{4\,c\,\sigma_{\rm T}\,\gamma_{\rm br}^2\,\mathcal{V}_{\rm gal}}\,\frac{\int_{\gamma}\,{\rm d}\gamma'\,\mathcal{I}(\gamma')}{\gamma^2\,U_{\rm B}\,(1+q\,F_{\rm KN})}. \tag{31}$$

This spectrum, in normalized units, is shown in Fig. 5 for $B_{\rm gal} = 3\,\mu$G (solid line) and 10 μG (dashed line). The shaded region indicates the energy range for which the turbulent re-acceleration effects (neglected here) are expected to become important. As can be noted, at low electron energies $\gamma < \gamma_{\rm KN}$, for which the inverse-Compton cooling in the Thomson regime dominates, the energy spectrum has a standard form $n_{\rm e}(\gamma) \propto \gamma^{-p}$ with $p = 2$, as expected in the case of the continuous injection of flat spectrum [$Q(\gamma < \gamma_{\rm br}) \propto$ constat] particles, followed by the $|\dot{\gamma}|_{\rm ic/T} \propto \gamma^2$ energy losses. However, for $\gamma > \gamma_{\rm KN}$ the electron spectrum flattens, as a result of the dominant inverse-Compton/Klein–Nishina cooling (see the most recent discussion in Moderski et al. 2005, and references therein), although in the case of $B_{\rm gal} = 10\,\mu$G this effect is relatively weak (the effective spectral index $p \sim 1.6$, to be compared with $p \sim 1.4$ for $B_{\rm gal} = 3\,\mu$G). Meanwhile, at $\gamma > \gamma_{\rm cr}$ the electron sepectral index in both cases increases to $p = 3.5$, as expected for the dominant synchrotron cooling $|\dot{\gamma}|_{\rm syn} \propto \gamma^2$ of the continuously injected steep-spectrum [$Q(\gamma > \gamma_{\rm br}) \propto \gamma^{-2.5}$] electrons.

With the evaluated electron energy distribution, one can find the energy spectrum of the resulting synchrotron and inverse-Compton emissions of the created pairs. In general, for the isotropic distribution of seed photons and particles, the respective luminosities can be simply

written as $[\varepsilon L_\varepsilon]_{\rm syn/ic} = 4\pi\,\mathcal{V}_{\rm gal}\,[\epsilon\, j_\epsilon]_{\rm syn/ic}$, where

$$[\epsilon\, j_\epsilon]_{\rm syn} = \frac{1}{2}\;\frac{n_{\rm e}(\gamma)\,\gamma}{4\pi}\,|\dot{\gamma}|_{\rm syn}\,m_{\rm e}c^2\Big|_{\gamma=\sqrt{(3/4)\,\epsilon_{\rm syn}\,(B_{\rm cr}/B)}}, \tag{32}$$

(assuming δ-approximation for the synchrotron emissivity; see Crusius & Schlickeiser 1986), $B_{\rm cr} \equiv 2\pi m_{\rm e}^2 c^3/h\,e = 4.4\times10^{13}$ G and

$$[\epsilon\, j_\epsilon]_{\rm ic} = \frac{3\,\sigma_{\rm T}\,m_{\rm e}c^3}{16\pi}\,\epsilon_{\rm ic}^2\int {\rm d}\gamma\int {\rm d}\epsilon\;\; n_{\rm e}(\gamma)\,n_{\rm rad}(\epsilon)\,\frac{\mathcal{F}_{\rm iso}(\gamma,\epsilon,\epsilon_{\rm ic})}{\epsilon\,\gamma^2}. \tag{33}$$

Here $\epsilon_{\rm syn/ic}$ denotes now the dimensionless energy of the synchrotron/inverse-Compton photons, electron energy distribution $n_{\rm e}(\gamma)$ is given by equation (31), seed photons' spectrum

$$n_{\rm rad}(\epsilon) = \frac{U_\epsilon}{\epsilon\,m_{\rm e}c^2} = \frac{\langle U_{\rm rad}\rangle}{m_{\rm e}c^2\,f_{\rm bol}}\,\epsilon^{-2}\,g(\epsilon) \tag{34}$$

is specified by equation (5), and finally

$$\mathcal{F}_{\rm iso}(\gamma,\epsilon,\epsilon_{\rm ic}) = 2\,\mathcal{P}\,\ln\mathcal{P} + \mathcal{P} + 1 - 2\mathcal{P}^2 + \frac{(\mathcal{K}\,\mathcal{P})^2\,(1-\mathcal{P})}{2\,(1+\mathcal{K}\,\mathcal{P})} \tag{35}$$

with

$$\mathcal{K} \equiv 4\epsilon\gamma \quad\text{and}\quad \mathcal{P} \equiv \frac{\epsilon_{\rm ic}}{4\epsilon\gamma\,(\gamma-\epsilon_{\rm ic})}, \tag{36}$$

where $1/4\gamma^2 \leqslant \mathcal{P} \leqslant 1$ (Blumenthal & Gould 1970). This leads to

$$[\epsilon L_\epsilon]_{\rm syn} = \frac{\tau\,L_{\rm inj}}{2\,\gamma_{\rm br}^2}\;\frac{\gamma\int_\gamma {\rm d}\gamma'\,\mathcal{I}(\gamma')}{1+q\,F_{\rm KN}}\Bigg|_{\gamma=\sqrt{(3/4)\,\epsilon_{\rm syn}\,(B_{\rm cr}/B)}}, \tag{37}$$

and

$$[\epsilon L_\epsilon]_{\rm ic} = \frac{9\,q\,\tau\,L_{\rm inj}}{16\,f_{\rm bol}\,\gamma_{\rm br}^2}\,\epsilon_{\rm ic}^2\int {\rm d}\gamma\int_{\max(\epsilon_{\rm min},\epsilon_{\rm low})}^{\min(\epsilon_{\rm max},\epsilon_{\rm up})} {\rm d}\epsilon\;\;\frac{\mathcal{F}_{\rm iso}(\gamma,\epsilon,\epsilon_{\rm ic})\,g(\epsilon)}{\epsilon^3\,\gamma^4\,(1+q\,F_{\rm KN})}\int_\gamma {\rm d}\gamma'\,\mathcal{I}(\gamma'), \tag{38}$$

where $\epsilon_{\rm low} \equiv \epsilon_{\rm ic}/4\gamma(\gamma-\epsilon_{\rm ic})$, and $\epsilon_{\rm up} \equiv \epsilon_{\rm ic}\gamma/(\gamma-\epsilon_{\rm ic})$. The evaluated luminosities are shown in Fig. 6, for $L_{\rm inj} = 10^{42}$ erg s^{-1} and the galactic magnetic fiel $B_{\rm gal} = 3$ μG (solid lines) and 10 μG (dashed lines). In the case of the inverse-Compton emission, spectral index in the photon energy range $\epsilon_{\rm ic} = 10^3$–10^6 (corresponding roughly to the electron energies $\gamma_{\rm KN} < \gamma < \gamma_{\rm br}$), is $\alpha_{\rm ic/KN} \sim 0.36$ for $B_{\rm gal} = 3$ μG, and $\alpha_{\rm ic/KN} \sim 0.45$ for 10 μG. These values are in agreement with the expected $\alpha_{\rm ic/KN} = p - 1$ for the appropriate electron spectral index $p = 1.4$ and 1.6, respectively (see a wide discussion in Moderski et al. 2005). At $\epsilon_{\rm ic} > 10^6$, the inverse-Compton emission breaks to $\propto \epsilon_{\rm ic}^{-2.6}$, again as expected in the case of a steep power-law electron continuum $\propto \gamma^{-3.5}$ at $\gamma > \gamma_{\rm br}$. In addition, Fig. 6 presents the 0.05–1000 MeV spectrum of the Cen A source as constrained by different instruments onboard *CGRO* (1991–1995; 'low' and 'intermediate' states; Steinle et al. 1998). As shown, the low-energy (1–100 GeV) flat-spectrum part of the predicted halo, if detected by the GLAST instrument in the future, could be spectrally distinguished from the (presumably nuclear) component observed by *CGRO*.

Fig. 6 indicates that almost all the energy injected to the elliptical host via annihilation of the nuclear γ-ray emission on the starlight photon field is re-emitted via the synchrotron emission at $\sim10^{13}$–10^{14} Hz frequencies, and via the inverse-Compton emission at $\gtrsim$0.1 TeV photon energies. Unfortunately, the secondary synchrotron photons have almost the same energy as the target starlight photons, and at the

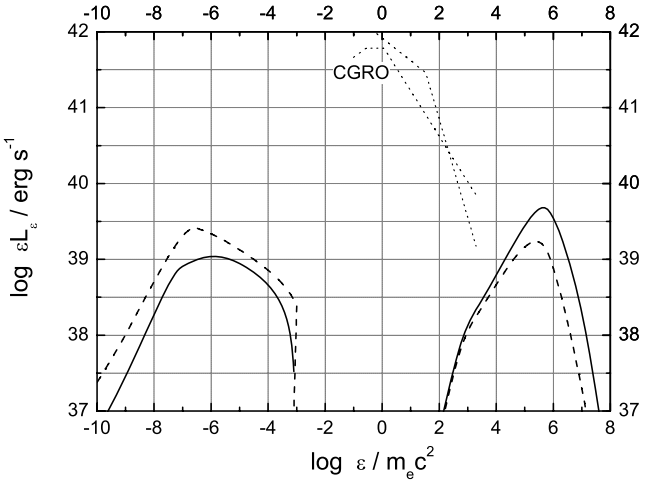

Figure 6. Synchrotron and inverse-Compton spectra of the electrons injected into the interstellar medium of the elliptical host for the galactic magnetic field 3 μG (solid lines) and 10 μG (dashed lines), and the injection luminosity $L_{\rm inj} = 10^{42}$ erg s^{-1}. Dotted lines indicate the 0.05–1000 MeV spectrum of the Cen A source as constrained by different instruments onboard *CGRO* (1991–1995; 'low' and 'intermediate' states; Steinle et al. 1998).

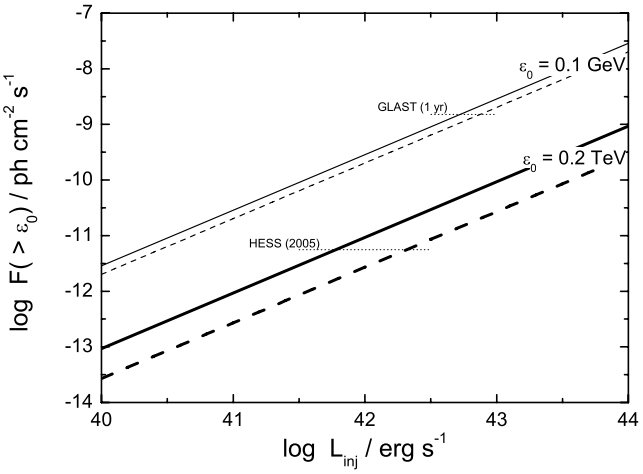

Figure 7. The expected photon fluxes of the Cen A halo for $\varepsilon_0 = 0.1$ GeV (thin lines) and $\varepsilon_0 = 0.2$ TeV (thick lines), corresponding to $B = 3$ and 10 μG (solid and dashed lines, respectively), as functions of the injection luminosity $L_{\rm inj}$. Horizontal dotted lines indicate HESS upper limit as given in Aharonian et al. (2005), and the expected GLAST sensitivity ($\sim 1.5 \times 10^{-9}$ ph cm^{-2} s^{-1} for one-year all-sky survey; Bloom 1996).

same time much lower total luminosity, and therefore are not likely to be directly observed. However, the secondary γ-ray emission, although also relatively weak, is more promising for the detection. In particular, the analysis presented above indicates that at high photon energies (>0.1 TeV) one should expect the photon flux from the galactic pair halo

$$F_{\rm iso} \sim \frac{[\varepsilon_0 L_{\varepsilon_0}]_{\rm ic}}{4\pi d_{\rm L}^2\, \varepsilon_0} \lesssim 10^{-11} \left(\frac{L_{\rm inj}}{10^{42}\,{\rm erg/s}} \right) \quad {\rm ph\,cm^{-2}\,s^{-1}}, \tag{39}$$

with the Cen A distance $d_{\rm L} = 3.4$ Mpc and $\varepsilon_0 = 0.2$ TeV. Note, that although the starlight radiation absorbs and reprocesses only a tiny ($\sim$1 per cent) fraction of the nuclear γ-ray emission, the small size of the resulting isotropic galactic pair haloes ($\sim 100\, r_{\rm b}$) make it quite easy to detect such structures. In fact, in the case of Cen A radio galaxy $100\, r_{\rm b}$ corresponds to roughly 4 kpc, or about 4 arcmin, which is still within the active nucleus-centred flux integration region of the HESS telescope. Thus, the estimate given in equation (21) can be directly compared with the HESS upper limits given in Aharonian et al. (2005). Such comparison implies that the time-averaged γ-ray output of the Cen A nucleus is indeed $L_{\rm inj} < 10^{42}$ erg s^{-1}, which is already a meaningful result. This demonstrates an important aspect of the presented analysis: observations of nearby AGNs at TeV photon energies can provide important constraints on the time-averaged VHE γ-ray fluxes produced in their active centres, even if these sources are not belonging to the blazar subclass (i.e. even if the nuclear portions of their jets are not inclined at small angles to the line of sight, and therefore their direct γ-ray emission is Doppler-hidden). Fig. 7 shows in more details the expected 0.19–5 TeV and 0.1–300 GeV photon fluxes of the inverse-Compton emission for the discussed Cen A galactic pair halo, together with the indicated HESS upper limit and the expected GLAST sensitivity ($\sim 1.5 \times 10^{-9}$ ph cm^{-2} s^{-1} for one-year all-sky survey; Bloom 1996). As is shown, future observations by HESS and GLAST will be able to put independent constraints on both the low- and high-energy spectral parts of the predicted halo.

4 DISCUSSION AND CONCLUSIONS

Several BL Lac objects are confirmed sources of variable and strongly Doppler-boosted TeV emission produced in the nuclear portions of their relativistic jets. It is more than probable that also many of the FR I radio galaxies, believed to be the parent population of BL Lacs, are TeV sources for which strongly Doppler-hidden nuclear γ-ray radiation may be only too weak to be directly observed (although see Aharonian et al. 2003; Beilicke et al. 2005, for the case of nearby FR I radio galaxy M 87 detected recently at TeV photon energies by HEGRA and HESS Cherenokov telescopes). Here we show, however, that about 1 per cent of the total time-averaged TeV radiation produced by the active nuclei of low-power FR I radio sources is inevitably absorbed and reprocessed by the photon–photon annihilation on the starlight photon field, and the following synchrotron/inverse-Compton emission of the created and quickly isotropized electron–positron pairs. Such a reprocessed isotropic radiation could be detected in the cases of at least a few nearby FR I radio galaxies, providing interesting constraints on the unknown parameters of the active nucleus and the elliptical host.

In the case of the Cen A radio galaxy considered in this paper, we found that the discussed mechanism can give distinctive radiative features due to the isotropic γ-ray emission of the electron–positron pairs injected by the absorption process into the interstellar medium of the elliptical host (its inner parts in particular, roughly within the radius of 4 kpc from the galactic centre), and inverse-Compton upscattering thereby starlight radiation to the $\leqslant$ TeV photon energy range. The resulting γ-ray halo is expected to possess a spectral peak at $\sim$0.1 TeV photon energies, preceded by a flat continuum due to the dominant Klein–Nishina cooling of the radiating electrons, and followed by a steep power law $\propto \epsilon_{\rm ic}^{-(\Gamma_\gamma + 0.5)}$, where Γ_γ is the photon index of the primary (nuclear) γ-ray emission. Such a halo should be strong enough to be detected and mapped by stereoscopic systems of Cherenkov telescopes like HESS, and, at lower photon energies, by GLAST.

All of the above findings should apply as well to the other nearby FR I sources. We note in this context that the kinetic power of the Cen A jet, $L_{\rm j} \sim 10^{43}$ erg s^{-1}, is rather low when compared to other FR I sources (e.g. $L_{\rm j} \gtrsim 10^{44}$ erg s^{-1} in the case of M 87 radio galaxy; Stawarz et al. (2006b), and references therein). Thus, other (though more distant) objects of the FR I type may posses more luminous isotropic haloes than Cen A analysed here. Indeed, taking the time- and angle-averaged nuclear γ-ray ($\sim$ TeV) luminosity $L_{\rm inj} \sim \eta_{\rm rad} L_{\rm j}$, where $\eta_{\rm rad}$ is the radiative efficiency, and the re-processed ($\gtrsim$0.1 TeV) luminosity $L_{\rm iso} \sim \tau L_{\rm inj}$ with $\tau \sim 0.01$ as estimated in this paper, one can find that modern Cherenkov telescopes with the available sensitivity limit 10^{-13} erg cm^{-2} s^{-1} will be able to detect the discussed haloes from the objects located within the radius roughly $d_{\rm L} \leqslant 100 \sqrt{(\eta_{\rm rad}/0.1)\,(L_{\rm j}/10^{44}\,{\rm erg\,s^{-1}})}$Mpc. Is it therefore possible to attribute the γ-ray flux detected recently from M 87 system (Aharonian et al. 2004) to the isotropic halo of its host galaxy? The answer is negative, since variability of this emission established on the time-scale of months and years (Beilicke et al. 2005) excludes any extended γ-ray emission sites.

ACKNOWLEDGMENTS

ŁS and MO were supported by MEiN through the research project 1-P03D-003-29 in 2005–2008. ŁS acknowledges also the ENIGMA Network through the grant HPRN-CT-2002-00321, and thanks Wystan Benbow as well as the referee, Marcus Böttcher, for helpful comments.

REFERENCES

Aharonian F. A., Atoyan A. M., Nagapetyan A. M., 1983, Astrophysics, 19, 187
Aharonian F. A., Coppi P. S., Völk H. J., 1994, ApJ, 423, L5
Aharonian F. A. et al., 2003, A&A, 403, L1
Aharonian F. A. et al., 2004, A&A, 421, 529
Aharonian F. A. et al., 2005, A&A, 441, 465
Bailey J., Sparks W. B., Hough J. H., Axon D. J., 1986, Nat, 322, 150
Beilicke M., Cornils R., Heinzelmann G., Raue M., Ripken J., Benbow W., Horns D., Tluczykont M., 2005, in Chen P., Bloom E., Madejski G., Patrosian V., eds, Proc. '22nd Texas Symposium on Relativistic Astrophysics', in press
Blandford R. D., Levinson A., 1995, ApJ, 441, 79
Bloom E. D., 1996, Space Sci. Rev., 75, 109
Blumenthal G. R., Gould R. J., 1970, Rev. Mod. Phys., 42, 237
Botti L. C. L., Abraham Z., 1993, MNRAS, 264, 807
Böttcher M., Schlickeiser R., 1997, A&A, 325, 866
Böttcher M., Mause H., Schlickeiser R., 1997, A&A, 324, 395
Burns J. O., Feigelson E. D., Schreier E. J., 1983, ApJ, 273, 128
Capetti A., Balmaverde B., 2005, A&A, 440, 73
Chiaberge M., Capetti A., Celotti A., 2001, MNRAS, 324, 33
Clarke D. A., Burns J. O., Norman M. L., 1992, ApJ, 395, 444
Colina L., de Juan L., 1995, ApJ, 448, 548
Coppi P. S., Blandford R. D., 1990, MNRAS 245, 453
Crusius A., Schlickeiser R., 1986, A&A, 164, 16
de Ruiter H. R., Parma P., Capetti A., Fanti R., Morganti R., Santantonio L., 2005, A&A, 439, 487
Dermer C. D., Schlickeiser R., 1994, ApJS, 90, 945
Eckart A., Cameron M., Rothermel H., Wild W., Zinnecker H., Rydbeck G., Olberg M., Wiklind T., 1990, ApJ, 363, 451
Golombek D., Miley G. K., Neugebauer G., 1988, AJ, 95, 26
Gould R. J., Schréder G. P., 1967, Phys. Rev., 155, 1404
Grindlay J. E., Helmken H. F., Brown R. H., Davis J., Allen L. R., 1975, ApJ, 197, 9
Hardcastle M. J., Worrall D. M., Kraft R. P., Forman W. R., Jones C., Murray S. S., 2003, ApJ, 593, 169
Heidt J., Tröller M., Nilsson K., Jäger K., Takalo L., Rekola R., Sillanpää A., 2004, A&A, 418, 813
Israel F. P., 1998, A&ARv, 8, 237
Jones D. L. et al., 1996, ApJ, 466, 63
Joy M., Lester D. F., Harvey P. M., Ellis H. B., 1988, ApJ, 326, 662
Kataoka J., Stawarz, Ł., Aharonian F., Takahara F., Ostrowski M., Edwards P. G., 2006, ApJ, 641, 158
Katarzyński K., Ghisellini G., Tavecchio F., Gracia J., Maraschi L., 2006, MNRAS, 368, 52
Knapp G. R., Bies W. E., van Gorkom J. H., 1990, AJ, 99, 476
Kraft R. P., Vázquez S. E., Forman W. R., Jones C., Murray S. S., Hardcastle M. J., Worrall D. M., Churazov E., 2003, ApJ, 592, 129
Lauer T. R. et al., 1995, AJ, 110, 2622
Marconi A., Pastorini G., Pacini F., Axon D. J., Capetti A., Macchetto D., Koekemoer A. M., Schreier E. J., 2006, A&A, 448, 921
Mathews W. G., Brighent F., 2003, ARA&A, 41, 191
Moderski R., Sikora M., Coppi P. S., Aharonian F., 2005, MNRAS, 363, 954
Morganti R., Robinson A., Fosbury R. A. E., di Serego Alighieri S., Tadhunter C. N., Malin D. F., 1991, MNRAS, 249, 91
Moss D., Shukurov A., 1996, MNRAS, 279, 229
Rowell G. P. et al., 1999, APh, 11, 217
Schlickeiser R., 1989, ApJ, 336, 243
Schlickeiser R., 2002, Cosmic Ray Astrophysics. Springer, Berlin
Sikora M., Begelman M. C., Rees M. J., 1994, ApJ, 421, 153
Sikora M., Madejski G., Moderski R., Poutanen J., 1997, ApJ, 484, 108
Silva L., Granato G. L., Bressan A., Danese L., 1998, ApJ, 509, 103

Stawarz Ł., Sikora M., Ostrowski M., 2003, ApJ, 597, 186
Stawarz Ł., Siemiginowska A., Ostrowski M., Sikora M., 2005, ApJ, 626, 120
Stawarz, Ł., Kneiske T. M., Kataoka J., 2006a, ApJ, 637, 693
Stawarz Ł., Aharonian F., Kataoka J., Ostrowski M., Siemiginowska A., Sikora M., 2006b, MNRAS, 370, 981
Steinle H. et al., 1998, A&A, 330, 97
Tingay S. J. et al., 1998, AJ, 115, 960
Urry C. M., Padovani P., 1995, PASP, 107, 803
Urry C. M., Scarpa R., O'Dowd M., Falomo R., Pesce J. E., Treves A., 2000, ApJ, 532, 816
Wagner S. J. et al., 1995, A&A, 298, 688
Wang J.-M., 2000, ApJ, 538, 181

APPENDIX A: OPACITY DUE TO THE 'DUST LANE'

The continuum far-infrared emission of NGC 5128, produced most likely by massive young stars and diffuse cirrus clouds (Joy et al. 1988; Eckart et al. 1990), is concentrated within the 'dust lane'. We model this feature as a thin disc, perpendicular to the jet axis, centred on the active nucleus, and extending up to radii $R_{\rm fir} \sim 4$ kpc (see Israel 1998). We also restrict the analysis to $\lambda_{\rm fir} = 100\,\mu$m radiation, for which we take the total observed (*IRAS*) flux ∼400 Jy (Golombek et al. 1988), corresponding to the luminosity $L_{\rm fir} \sim 1.6 \times 10^{43}$ erg s^{-1}. The number density of the far-infrared photons, assumed to be uniformly distributed within the 'dust-lane', is then

$$n_{{\rm fir},\epsilon}(\xi, \Omega) = \frac{L_{\rm fir}}{8\,\pi^2\,R_{\rm fir}^2\,\epsilon_{\rm fir}\,m_{\rm e}c^3}\,\delta(\epsilon - \epsilon_{\rm fir}). \tag{A1}$$

The appropriate optical depth for the photon–photon annihilation, analogous to the one given by equation (13), can be then evaluated as

$$\tau(\epsilon_\gamma) = \frac{L_{\rm fir}\,r_{\rm b}}{8\,\pi^2\,R_{\rm fir}^2\,\epsilon_{\rm fir}\,m_{\rm e}c^3}\int_0^{\xi_{\rm t}} {\rm d}\xi \int_{\cos[\arccot(\xi/100)]}^{+1} {\rm d}\varpi\ \ (1-\varpi)\ \ \sigma_{\gamma\gamma}(\epsilon_\gamma, \epsilon_{\rm fir}, \varpi). \tag{A2}$$

This optical depth is shown in Fig. A1 (solid line) together with the optical depth due to the starlight emission of the elliptical host evaluated previously (dotted line). As shown, opacity due to the dust lane is much smaller than the opacity due to the elliptical host (because of the different spatial distribution of the target photons), and in addition regards only very high energies (>100 TeV) of the primary γ-rays.

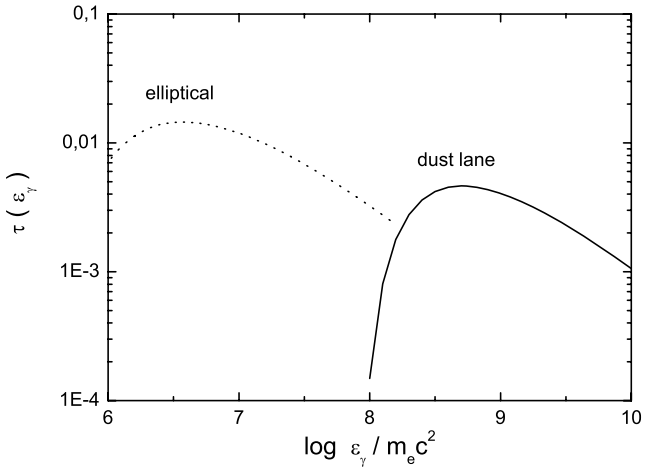

Figure A1. Optical depth for the photon–photon annihilation due to the dust lane (solid line) and the elliptical host (dotted line).

This paper has been typeset from a TEX/LATEX file prepared by the author.